Simulation of the size-composition distribution of atmospheric nanoparticles over Europe

David Patoulias[1,2], Christos Fountoukis[2,3], Ilona Riipinen[4], Ari Asmi[5], Markku Kulmala[5], and Spyros N. Pandis[1,2,6]

[1] Department of Chemical Engineering, University of Patras, Patras, Greece

[2] Institute of Chemical Engineering Sciences, Foundation for Research and Technology Hellas (FORTH/ICE-HT), Patras, Greece

[3] Qatar Environment & Energy Research Institute, Hamad Bin Khalifa University, Doha, Qatar

[4] Department of Applied Environmental Science & Bert Bolin Centre for Climate Research, Stockholm University, Stockholm, Sweden

[5] Department of Physics, University of Helsinki, P.O. Box 64, 00014, Helsinki, Finland.

[6] Department of Chemical Engineering, Carnegie Mellon University, Pittsburgh, PA 15213, USA.

Abstract

PMCAMx-UF, a three-dimensional chemical transport model focusing on the simulation of the ultrafine particle size distribution and composition has been extended with the addition of the volatility basis set (VBS) approach for the simulation of organic aerosol (OA). The model was applied in Europe to quantify the effect of secondary semi-volatile organic vapors on particle number concentrations. The model predictions were evaluated against field observations collected during the PEGASOS-2012 campaign. The measurements included both ground and airborne measurements, from stations across Europe and a Zeppelin measuring above Po-Valley. The ground level concentrations of particles with diameter larger than 100 nm (N_{100}) were reproduced with a daily normalized mean error of 40% and a daily normalized mean bias of -20%. PMCAMx-UF tended to overestimate the concentration of particles with diameter larger than 10 nm (N_{10}) with a daily normalized mean bias of 75%. The model was able to reproduce within a factor of two 85% of the N_{10} and 75% of the N_{100} Zeppelin measurements above ground. The condensation of organics led to an increase (50-120%) of the N_{100} concentration mainly in central and northern Europe, while the N_{10} concentration decreased by 10-30%. Including the VBS in the PMCAMx-UF improved its ability to simulate aerosol number concentration compared to simulations neglecting organic condensation on ultrafine particles.

1. Introduction

New particles are introduced in the atmosphere by two major processes; direct emission from multiple sources and nucleation from low volatility vapors. Nucleation and subsequent growth of new particles have been observed in a variety of environments worldwide (Kulmala et al., 2004), representing a significant source of aerosol number. Fresh particles formed by nucleation can either be lost through coagulation with pre-existing larger particles or grow through condensation of vapors (e.g. sulfuric acid, ammonia, organics, and nitric acid) to larger sizes (Adams and Seinfeld, 2002) and become cloud condensation nuclei (CCN), thereby increasing the cloud droplet number concentration (Adams and Seinfeld, 2002). Thus, nucleation and subsequent growth by condensation can be an important source of CCN (Makkonen et al., 2009; Merikanto et al., 2009; Pierce and Adams, 2009; Wang and Penner, 2009; Yu and Luo, 2009). Considerable uncertainty arises from the partial understanding of the identity of the species involved in the growth of these nuclei (Kulmala et al., 2004; Kerminen et al., 2012). Field measurements (Eisele and McMurry, 1997; Weber et al., 1998, 1999) and model simulations (Kulmala et al., 2000; Pirjola and Kulmala, 2001; Anttila and Kerminen, 2003) indicated that the condensation of sulfuric acid alone is often not sufficient to justify the observed growth rates of fresh particles (Riipinen et al., 2011). Organics dominate particle growth in a lot of environments, but sulfuric acid and ammonia also play an important role in sulfur rich areas (Stanier et al., 2004; Yue et al., 2010). Growth of new particles has been attributed to the condensation of organic species (Kulmala et al., 1998; Anttila and Kerminen, 2003; Kerminen et al., 2000), heterogeneous reactions (Zhang and Wexler, 2002), or ion-enhanced condensation (Laakso et al., 2002).

Secondary organic aerosol (SOA) comprises a major mass fraction (20-90%) of sub-micrometer particulate matter in many locations around the globe (Jimenez et al., 2009). Even though organic aerosol (OA) has been the subject of numerous studies (Hallquist et al., 2009), its chemical composition remains uncertain, making it one of the least understood components of atmospheric aerosols, due to the large number of different atmospheric organic compounds (Goldstein and Galbally, 2007).

Atmospheric OA composition continuously evolves with time as a result of various chemical reactions (Kanakidou et al., 2005). The semi-volatile products which are produced from the gas-phase oxidation of volatile organic compounds (VOCs) can afterwards condense to

the particulate phase. The volatility bases set (VBS) framework describes the volatility distribution of OA compounds (Donahue et al., 2006) using logarithmically spaced bins of the effective saturation concentration, C^* (in μg m^{-3}) at 298 K, to classify atmospheric organic species. This framework has been tested in three-dimensional regional (3-D) chemical transport models (CTMs), and appears to perform well for simulations of aerosol mass distributions (Gaydos et al., 2007; Karydis et al., 2007; Murphy et al., 2009; Tsimpidi et al., 2010; Fountoukis et al., 2011, 2014).

A new 3-D CTM, PMCAMx-UF, with detailed aerosol microphysics was developed by Jung et al. (2010), and has been used for simulations over the US and Europe (Fountoukis et al., 2012; Baranizadeh et al., 2016). For the US domain, the first comparison of the model and the measurements in Pittsburgh was encouraging; this evaluation focused on the frequency, timing, and strength of nucleation events (Jung et al., 2010). Applications in Europe compared model predictions against size distribution measurements from seven sites (Fountoukis et al., 2012). The model was capable of reproducing more than 70% of the hourly number concentrations of particles larger than 10 nm (N_{10}) within a factor of 2. However, the concentration of particles larger than 100 nm (N_{100}, the number of particles that can act as CCN) was underpredicted by 50%. Even at sites where the sulfate to OA mass ratio was high (e.g., Melpitz), the nanoparticle growth rates was underpredicted, but with smaller errors as compared with sites with relatively less sulfate. These problems were caused mainly by insufficient organic vapor condensation (Fountoukis et al., 2012), as the model did not explicitly include SOA condensation on particles. Based on observations from two background sites, Riipinen et al. (2011) estimated that roughly half of the condensed organic mass should contribute to nanoparticle growth in order to explain the observed aerosol growth rates.

Patoulias et al. (2015) developed a new aerosol dynamic model, DMANx (Dynamic Model for Aerosol Nucleation), that simulates aerosol size/composition distribution, and includes the condensation of organic vapors on nanoparticles using the VBS framework. Simulations were performed for the sites of Hyytiälä (Finland) and Finokalia (Greece); two locations with different organic sources. Patoulias et al. (2015) investigated the effect of condensation of organics and chemical aging reactions of SOA precursors on ultrafine particle growth and particle number concentration during a typical springtime nucleation event in both locations. At the Finokalia site, the simulations suggested that the organics play a complementary role in new particle

growth, contributing 45% to the total mass of new particles. Condensation of organics increased the N_{100} by 13% at Finokalia, and 25% at Hyytiälä during a typical spring day with nucleation.

The overall objective of this work is to examine the effect of the condensation of secondary organic vapors (products of the oxidation of VOCs and of the intermediate volatility organic compounds; IVOCs) on particle number concentrations. Our hypothesis is that simulation of the corresponding interactions improves the ability of CTMs to reproduce ambient observations of the aerosol number distribution. Organic condensation can play a much more complex role than simply helping in the ultrafine particle growth. It increases the condensational and coagulation sinks thus reducing nucleation rates and increasing coagulation rates. Given the complexity and the nonlinearity of these interactions the net effect of organic condensation on particle number concentrations is by no means obvious.

We extended the 3-D CTM PMCAMx-UF (Fountoukis et al., 2012; Jung et al., 2010), which originally assumed that ultrafine particles can grow only by condensation of sulfuric acid and ammonia as well as by coagulation. The updated version of PMCAMx-UF includes the condensation of organic vapors on ultrafine particles using the VBS framework. We evaluated the model by comparing its predictions to surface-based high-time-resolution measurements from 16 stations in Europe and airborne measurements from the PEGASOS Zeppelin campaign over the Po Valley, in Italy.

2. Model description

PMCAMx-UF is a three-dimensional CTM that simulates the aerosol number size distribution, in addition to the mass/composition size distribution (Jung et al., 2010; Fountoukis et al., 2012). PMCAMx-UF is based on the framework of PMCAMx (Gaydos et al., 2007; Karydis et al., 2007), describing the processes of horizontal and vertical advection, emissions, horizontal and vertical dispersion, wet and dry deposition, aqueous and aerosol phase chemistry, as well as aerosol dynamics. For the simulation of aerosol microphysics, PMCAMx-UF uses the updated DMANx model of Patoulias et al. (2015), which simulates the processes of coagulation, condensation/evaporation and nucleation, assuming an internally mixed aerosol. DMANx uses the two-moment aerosol sectional (TOMAS) algorithm (Adams and Seinfeld, 2002; Jung et al., 2006). A key feature of TOMAS is its ability to track two independent moments of the aerosol size distribution for each size bin; the aerosol number and mass concentration. The aerosol size

distribution is described with 41 size sections with the lowest boundary at 3.75×10^{-25} kg dry aerosol mass per particle. That corresponds approximately to a dry diameter of 0.8 nm. The particle density in each bin is calculated and updated continuously as a function of the corresponding composition. Each successive boundary has double the mass of the previous one to facilitate the simulation of coagulation (Tzivion et al., 1987; 1989).

The particle components modeled include sulfate, ammonium, nitrate, sodium, chloride, crustal material, water (H_2O), elemental carbon (EC), primary organic aerosol (POA) and four SOA components. The TOMAS algorithm simulates the evaporation, condensation of sulfuric acid (H_2SO_4), ammonia (NH_3) and organics, independently.

2.1 Nucleation parameterizations

PMCAMx-UF has the option of using a number of nucleation treatments (Fountoukis et al., 2012; Baranizadeh et al., 2016). In this work, the nucleation rate was calculated using a scaled ternary nucleation parameterization based on the original expressions of Napari et al. (2002) and the binary parameterization of Vehkamäki et al. (2002), if the NH_3 concentration is below a threshold value of 0.01 ppt. The original NH_3-H_2SO_4-H_2O parameterization had predicted successfully the presence or lack of nucleation events (Gaydos et al., 2005) in sulfur rich environments. However, it overpredicted ultrafine number concentrations during nucleation events (Fountoukis et al., 2012; Jung et al., 2008, 2010), and thus a scaling factor of 10^{-6} was applied to the nucleation rate following the suggestions of Fountoukis et al. (2012). The critical nucleus is assumed to consist of roughly two molecules of sulfuric acid and two molecules of ammonia consistent with its assumed size (Napari et al., 2002).

2.2 Gas-phase chemistry

The gas phase chemistry mechanism in PMCAMx-UF was updated in this work to the SAPRC chemical mechanism (Carter, 2000; Environ, 2003), which includes 211 reactions of 56 gases and 18 free radicals. The SAPRC version used here includes five lumped alkanes (ALK1-5), two lumped olefins (OLE1-2), two lumped aromatics (ARO1-2), isoprene (ISOP), a lumped monoterpene (TERP) and a lumped sesquiterpene species (SESQ). OLE1 contains all the terminal alkenes, while OLE2 represents all the internal and cyclic alkenes. All lumped VOCs

with the exception of ALK1-3 are considered as SOA precursors (Lane et al., 2008a, b; Tsimpidi et al., 2010).

2.3 Coagulation

Coagulation of particles in the atmosphere is an important sink of aerosol number, but is also a mechanism by which freshly nucleated particles grow to larger sizes (Adams and Seinfeld, 2002). The TOMAS algorithm is used for the simulation of coagulation. Following Adams and Seinfeld (2002), TOMAS assumes that the particles coagulate via Brownian diffusion and the effects of gravitational settling and turbulence are neglected.

2.4 Particle number/mass emissions

The particle emissions were based on the pan-European anthropogenic particle number emission inventory (Denier van der Gon et al., 2009; Kulmala et al., 2011) and the carbonaceous aerosol inventory (Kulmala et al., 2011) developed during the EUCAARI (European Integrated project on Aerosol, Cloud, Climate, and Air Quality Interactions) project. The resulting number/mass inventory includes both number emissions and consistent size-resolved composition for particles over the size range of 10 nm to 10 μm. Hourly gridded anthropogenic and biogenic emissions included both gases and primary particulate matter. The natural emissions include both particulate matter and gases and combine three different data sets: emissions from ecosystems based on the Model of Emissions of Gases and Aerosols from Nature (MEGAN; Guenther et al., 2006), marine emissions based on the model of O'Dowd et al. (2008), and wildfire emissions (Sofiev et al., 2008a, b). MEGAN uses as inputs the plant functional type, the leaf area index, various chemical species emission factors and weather data provided by the weather research and forecasting model (WRF) (Skamarock et al., 2005). Since sea surface covers a considerable portion of the domain, the marine aerosol emission model developed by O'Dowd et al. (2008) was also used. Wind speed fields from WRF and chlorophyll-a concentrations were used as inputs of the marine aerosol model. VOCs were speciated based on the approach proposed by Visschedijk et al. (2007). Anthropogenic gas emissions included land emissions from the GEMS (global and regional Earth-system monitoring using satellite and in-situ data) dataset (Visschedijk et al., 2007). International shipping, industrial, domestic, agricultural, and traffic

aerosol emission sources were included in the anthropogenic inventory (Denier van der Gon et al., 2009; Kulmala et al., 2011).

2.5 Condensation/Evaporation

Condensation of gas-phase species to existing aerosol particles is an important source of aerosol mass and a means by which small particles grow to CCN sizes. The TOMAS algorithm was used for the simulation of condensation/evaporation of sulfuric acid, ammonia and organic vapors, using the wet diameters of the particles (Gaydos et al., 2005).

Sulfuric acid is assumed to be in pseudo-steady state in DMANx. This pseudo steady-state approximation (PSSA) for sulfuric acid proposed by Pierce and Adams (2009) increases the computational speed with a small loss in accuracy. Jung et al. (2010) evaluated the performance of PSSA for sulfuric acid in DMAN against a 4^{th} order Runge-Kutta algorithm and showed that PSSA was accurate and computationally efficient. Condensation of ammonia was simulated following the approach described by Jung et al. (2006). Ammonia condensation on the ultrafine particles ends when sulfate is fully neutralized to ammonium sulfate.

Nitric and hydrochloric acid partition to particles in the accumulation and coarse modes in DMAN as nitrate and chloride, respectively. This partitioning is simulated using the bulk equilibrium approach. At each time step the amount of nitric acid and hydrochloric acid transferred between the gas and aerosol phases is determined by applying the aerosol thermodynamic equilibrium model ISORROPIA (Nenes et al., 1998). This amount is then distributed over the aerosol size distribution by using weighting factors for each size section based on their effective surface area (Pandis et al., 1993). This treatment ensures that the appropriate amount is transferred to the larger particles; however it cannot describe accurately any potential transfer of these acids to the nucleation mode. This simplification dramatically reduces the computational burden with a minimal loss of accuracy, since ultrafine particle growth is governed by low-volatility compounds.

2.6 Secondary organic aerosol formation

Gas-phase oxidation of VOCs produces semi-volatile products that can then condense to the particle phase. The VBS framework (Donahue et al., 2006) used in PMCAMx-UF describes the volatility distribution of OA compounds using logarithmically spaced bins, characterized by an

effective saturation concentration, C^* (in μg m^{-3}). SOA components partition between the aerosol and gas phases, and can be formed from anthropogenic (aSOA) and biogenic (bSOA) precursors. SOA partitioning was simulated using 4 volatility bins ($1 – 10^3$ μg m^{-3} at 298 K). We assume an average molecular weight of 200 g mol^{-1} for SOA, and an effective enthalpy of vaporization of 30 kJ mol^{-1} (Pathak et al., 2007; Stanier et al., 2007). The partitioning of OA between the gas and particulate phases is simulated dynamically (Patoulias et al., 2015).

The SOA yields used in the updated version of PMCAMx-UF are based on the NO_x-dependent yields of Murphy at al. (2009). The current work focuses on the effect of the formation of semi-volatile organic aerosol on particle number concentrations. The role of later generation reactions (known as chemical aging) and also the formation of low volatility (LVOC) and extremely low-volatility organic compound (ELVOC) formation (Ehn et al., 2014; Tröstl et al., 2016) is rather complex and will be the topic of future work.

2.7 Meteorological input fields

Meteorological inputs to PMCAMx-UF included horizontal wind components, vertical diffusivity, temperature, pressure, water vapor, clouds and rainfall. The meteorological model WRF (Skamarock et al., 2005) was used to create the above inputs. WRF was driven by geographical and dynamic meteorological data (historical data generated by the Global Forecast System). Each layer of PMCAMx-UF was aligned with the layers used in WRF. The WRF simulation was periodically re-initialized (every 3 days) with observed conditions to ensure accuracy in the corresponding fields that were used as inputs in PMCAMx-UF, for 34 days from June 5 to July 8, 2012. The three-day re-initialization has been chosen because of its simplicity and the fact that the corresponding WRF predictions remain consistent with all the measurements. The measurements are pre-processed by the WPS (WRF Preprocessing System) package, which provides each atmospheric and static field with fidelity appropriate to the chosen grid resolution of the model. The performance of WRF for Europe against observed meteorological variables has been the topic of several studies (Jimenez-Guerrero et al., 2008; de Meij et al., 2009; Im et al., 2010; Argueso et al., 2011; Garcia-Diez et al., 2012) with all of them showing good performance.

3. Model Application and Measurements

The PMCAMx-UF modeling domain in this application covered a 5400 × 5832 km^2 region in Europe (Fig. 1), with 150 cells in the x- and 162 cells in the y- direction, with a 36 × 36 km grid resolution and 14 vertical layers (the height of each layer can be found in the Supplementary Information, Table S1) extending up to approximately 7.5 km. PMCAMx-UF was set to perform simulations on a rotated polar stereographic map projection.

The first two days of each simulation were excluded from the analysis to minimize the effect of the initial conditions on the results. The initial conditions affect the predictions for a period similar to the average residence time of the pollutants in the modeling domain. Given that this is a regional simulation, this period is significantly shorter than the lifetime of the particles in the atmosphere. Based on our tests two days are indeed sufficient for the model to "forget" the initial conditions and for emissions and chemistry to take over. The initial concentrations used are low to further decrease their impact on the results (Supplementary Information, Table S2).

Constant very low values have been used for the boundary conditions (Table S2) so that the predicted particle number concentrations over Europe are determined for all practical purposes by the emissions and corresponding processes simulated by the model. The effect of these boundary conditions on the predicted number concentrations is discussed in a subsequent section.

An intensive field campaign took place in Europe, as part of the Pan-European-Gas-AeroSOl-climate-interaction Study (PEGASOS) project, for 34 days from June 5 to July 8, 2012. Measurements of aerosol size distribution from the Aerosols, Clouds, and Trace gases Research Infra-Structure Network (ACTRIS), Chemistry-Aerosol Mediterranean Experiment (ChArMEx) and the German Ultrafine Aerosol Network (GUAN) network are also available for the same period. The model results were compared against measurements in ground sites (Fig. 1): Birkenes (Norway), Hyytiala (Finland), Aspvreten (Sweden), Vavihill (Sweden), K-Puszta (Hungary), Ispra (Italy), San Pietro Capofiume (Italy), Corsica (France), Patras (Greece), Finokalia (Greece), Thessaloniki (Greece), Mace Head (Ireland), Hohenpeissenberg (Germany), Melpitz (Germany), Waldhof (Germany) and Schneefernerhaus (Germany). The measurements are available in the European Supersites for Atmospheric Aerosol Research (EUSAAR), ChArMEx (charmex.lsce.ipsl.fr) and EBAS databases (ebas.nilu.no). Particle size distribution measurements at all sites were made using either a Differential Mobility Particle Sizer (DMPS)

or a Scanning Mobility Particle Sizer (SMPS). Information about all stations can be found in the Supplementary Information (SI, section S1).

The airborne measurements acquired by a Zeppelin were part of the PEGASOS project over the Po Valley in Italy. The Po Valley region is situated between the Alps in the north and the Apennines Mountains in the south–southwest. The mountains surround the valley on three sides and strongly modify both the local and regional air flow patterns in the area (Sogacheva et al., 2007). High levels of pollutants are often observed in the region due to the industrial, agricultural, and other anthropogenic emissions. In addition, the emissions from ship traffic on the Adriatic Sea (Hamed et al., 2007) and long-range transport from central-eastern Europe are possible sources of pollutants in the region (Sogacheva et al., 2007). A scanning mobility particle sizer (SMPS) was used to measure the number size distribution of particles in the size range of 10 to 430 nm.

4. Results

4.1 Base Case simulation

Figure 2 shows the base case PMCAMx-UF predictions of ground level average number concentration for all particles (N_{tot}) and for particles with diameters above 10 nm (N_{10}), 50 nm (N_{50}), and 100 nm (N_{100}), during June 5 to July 8, 2012 (34 days). The N_{50} and N_{100} concentrations are often used as proxies for CCN-related aerosol number concentrations (Fountoukis et al., 2012). The N_{10} can be directly compared against the differential mobility particle sizer (DMPS) or SMPS measurements. On a domain average basis, the model predicted for the ground level N_{tot} = 6500 cm^{-3}, N_{10} = 3800 cm^{-3}, N_{50}= 1550 cm^{-3} and N_{100} = 520 cm^{-3} during the simulated period. High N_{tot} and N_{10} are predicted in areas with frequent nucleation events and also areas with high primary particle number emissions. Average N_{tot} concentrations exceeding 20,000 cm^{-3} were predicted over Bulgaria, Bosnia, southern Romania, Turkey, Germany, Poland, Holland, Portugal, northern Spain, eastern UK, northern Italy, and central Russia. On the other hand, N_{50} and N_{100} are also affected by secondary particulate matter production. The highest N_{50} and N_{100} concentrations are predicted over the Mediterranean, mainly in areas near southern Spain, southern Italy and Greece.

An additional simulation, without taking into account the condensation of organics was also performed. The average fractional increase of N_x, f_{Nx}, due to the condensation of organic species is defined as:

$$f_{Nx} = \frac{N_x(\text{with organics}) - N_x(\text{without organics})}{N_x(\text{without organics})} \quad (4.1)$$

where x is 10, 50, 100 nm or total.

Predictions of f_{Nx} are shown in Fig. 3. The average fractional changes are -0.02, -0.05, 0.15 and 0.33 for the N_{tot}, N_{10}, N_{50} and N_{100}, respectively. The condensation of organics was predicted to decrease the total number concentration N_{tot} over most continental Europe. The largest decrease was approximately 50%. This rather counterintuitive result is due to the increase of both the condensation and coagulation sinks as SOA is formed. These effects dominated over the faster growth of fresh nuclei or other nanoparticles to larger sizes that tend to slow down their coagulation rate and increase their lifetime. In the other extreme an increase of N_{tot} of approximately 60% was predicted over the eastern UK. In this area organic condensation does lead to higher number concentrations. The predicted N_{10} also decreased between 15-30%, due to organic condensation over most of Europe. The minimum value of f_{N10} was about -0.30 over Serbia, while the maximum f_{N10} was about 0.35 over eastern UK. On the other hand, the condensation of organics increased the N_{50} over the whole domain. The increase was 40-80% over Scandinavia and northern Russia. The condensation of semi-volatile organic vapors results in an increase of N_{100} by 70-150% over northern Scandinavia and northwestern Russia according to PMCAMx-UF.

The absolute increase in particle number concentration (ΔN_x) due to the organic condensation is defined as:

$$\Delta N_x = N_x \text{ (with organics)} - N_x \text{ (without organics)} \quad (4.2)$$

where x is 10, 50, 100 nm or total.

N_{tot} decreased over Turkey, central and Eastern Europe, and Balkans by 2000 to 5000 cm^{-3} while it increased over the eastern UK by roughly 3000 cm^{-3} (Fig. S1 in Supplementary Information). The highest reduction of N_{tot} was approximately 15000 cm^{-3} over Hungary and central Turkey. The predicted ΔN_{10} over central Europe was in the range of -1000 to -3000 cm^{-3}. The maximum reduction of N_{10} was equal to 3600 cm^{-3} over Hungary while its maximum increase was 6500 cm^{-3} over eastern UK. The N_{50} increased due to the condensation of organics

over Italy, central Russia, Holland, Ukraine, eastern Mediterranean, the coast of Algeria and Spain by 500 - 2000 cm^{-3}. N_{100} increases from 300 to 800 cm^{-3} over the Mediterranean and south Russia. The maximum N_{100} increase was about 2000 cm^{-3} over Malta and southern Italy. The corresponding changes of the concentrations of particles with diameters between 10 nm and 50 nm ($N_{10\text{-}50}$) and between 50 nm and 100 nm ($N_{10\text{-}50}$) are shown in Figure S2.

4.2 Evaluation of extended PMCAMx-UF

The predicted daily average concentrations of particles larger than 10, 50 and 100 nm are compared to the corresponding observations in all ground stations in Fig. 4. Around 65% of the observed N_{10} observations were reproduced within a factor of 2 by PMCAMx-UF, with the model tending to overestimate the corresponding concentrations. The model performed even better for N_{50} reproducing 80% of the measurements within a factor of 2. PMCAMx-UF presented a tendency to underestimate the N_{100}, levels but still reproduced 70% of the data, within a factor of 2. The model does a good job in capturing the observed variability in all size ranges and also appears to reproduce the observations at the low concentration levels.

The prediction skill metrics of PMCAMx-UF, when compared against the daily average measurements from the 16 stations, are summarized in Tables 1-3. The average normalized mean error (NME) for N_{10} was 90% and the normalized mean bias (NMB) was 75%. The N_{10} was overestimated in most locations with the exception of Hyytiala, San Pietro Capofiume, and Hohenpeissenberg. The normalized mean bias was less than 30% in K-Puszta, Melpitz and Patras. The model really overpredicted N_{10} (NMB>100%) in several stations in Northern Europe (Aspvreten, Birkenes, Vavihill), some coastal locations (Corsica and Mace Head), two German sites (Waldhod and Schneefernerhaus) and the Thessaloniki site in northern Greece. The overall NMB and NME for N_{50} were 25% and 50%, respectively. The N_{50} NMB was less than 50% in 14 stations, with only Aspvreten and Thessaloniki being exceptions. In these 14 stations the corresponding error was less than 70%. Finally, the N_{100} was underpredicted in all stations with the exception of two Greek sites (Thessaloniki and Finokalia). However, this underprediction was less than 30% in 9 out of the 14 sites. Overall, the NMB for N_{100} was -20% and the NME for N_{100} was 40% for the simulation with organics.

Figures 5 and S3-S5 show measured and predicted average diurnal profiles of N_{10}. In Hyytiala, Patras and Hohenpeissenberg, the observed diurnal profiles of N_{10} were flat, and the

predicted diurnal profiles of N_{10} were close to the observations. In Melpitz and San Pietro Capofiume, the observed and predicted N_{10} increased at noon due to nucleation. In K-Puszta, Ispra, Birkenes, Aspvreten, Vavihill, Thessaloniki, Schneefernerhaus, Finokalia, Corsica and Waldhof, the model overpredicted N_{10}.

One of the potential explanations for the overprediction of N_{10} is the corresponding overprediction in the frequency of nucleation. Figure 6 shows the predicted and measured nucleation frequency for the 16 stations during the 34 simulation days. The criteria proposed by Dal Maso et al. (2005) were used for the categorization of a day as a nucleation event. The nucleation frequency was defined as the ratio of the number of days characterized as nucleation events to the total number of days.

The observed nucleation frequency varied dramatically in the 16 sites from over 90% in San Pietro Capofiume to less than 10% in Patras. PMCAMx-UF reproduced this wide range (Fig. 6) with the predicted nucleation frequency being within 20% of the observed one in 12 out of the 16 stations. The model tends to overpredict nucleation frequency with the most significant errors in two coastal stations in the Mediterranean (Corsica and Patras) and two stations in Scandinavia (Birkenes and Aspreveten). This suggests that overpredicted nucleation frequency can explain part of the N_{10} overprediction in at least three (Corsica, Birkenes and Aspreveten) out of the eight stations.

The overprediction of N_{10} could be also due to the low surface area of the particles resulting in lower condensation and coagulation rates. The capability of the existing aerosol population to remove vapors and freshly formed particles can be described by the condensational sinks (CS) (Dal Maso et al., 2005). The model undepredicted the measured the condensational sink in most of the sites. In Corsica the model overpredicted the condensation sink, while in Thessaloniki, Birkenes and Aspreveten the model is in good agreement with the measurements (Fig. 7). Summarizing, the errors in N_{10} are caused by the high predicted nucleation rate at Aspvreten, Birkenes, Schneefernerhaus, Thessaloniki and Vavihill and they are, at least partially, due to low predicted condensation sink at Ispra, K-Puszta, Mace Head and Melpitz. At Corsica, the overprediction of N_{10} is due to errors in both the predicted nucleation rates and the condensation sink.

The average diurnal profiles of N_{100} for all sites are shown in Fig. 8 and Figures S6-S8. The model reproduced satisfactorily the average observed of N_{100} in the Mediterranean (Corsica, San

Pietro Capofiume, Patra and Finokalia) with the exceptions of Thessaloniki, where PMCAMx-UF overestimated N_{100} for the most hours of the day.

In northern Europe, the predicted N_{100} was in general below the observed N_{100}. The maximum underprediction of N_{100} was observed in Hyytiala, Mace Head, and Melpitz. This indicated that the concentration of large particles was lower than observed, and therefore the condensation sink was also lower (Fig. 7). This underprediction is probably due to a combination of lower primary particles emissions and lower growth rates of the particles. The PMCAMx-UF predictions for Hyytiala and Mace Head are also quite sensitive to the boundary conditions used. Underestimation of the corresponding values could contribute to the N_{100} underpredictions in these locations. The low prediction of organic aerosol is causing the underprediction of N_{100} in Patras and San Pietro Capofiume.

4.3 Comparison to aerosol composition measurements

The PMCAMx-UF predictions can be evaluated during that period using available PM_1 measurements from Aerosol Mass Spectrometers in 4 stations (Bologna and San Pietro Capofiume in Italy as well as Finokalia and Patras in Greece) and filter $PM_{2.5}$ measurements from 12 additional stations in Europe (Table S3).

In Italy and Greece, the model reproduces the observations of inorganic aerosol components (sulfate, nitrate, ammonium) reasonably well (e.g., errors in the average concentrations of less than 0.5 μg m^{-3} in the Italian sites), but it tends to underpredict the organic aerosol concentrations (Table S4). For example, the OA in San Pietro Capofiume is underpredicted by 40%. This underprediction of the organics is the major reason for the underprediction of the condensational sink shown in Figure 7 and is probably due to our assumptions about the chemical aging of the anthropogenic SOA. Based on previous work with the sister model PMCAMx (Fountoukis et al., 2011; 2014) in Europe, the chemical aging processes, that are not simulated in this version of PMCAMx-UF, should be able to explain a significant fraction of the missing OA. The role of these processes, the detailed evaluation of PMCAMx PM_1 mass and composition predictions during the PEGASOS campaigns and the sensitivity of the model to chemical aging parameterizations are the main topics of on-going work.

For the rest of Europe we have used measurements available in the European Supersites for Atmospheric Aerosol Research (EUSAAR) and EBAS databases (ebas.nilu.no) for stations that had available data for more than 15 days during the simulation period. Concerning the inorganic components, the model reproduced the sulfate measurements within 0.5 μg m^{-3} (Table S6). On the other hand, it has a tendency to overestimate the ammonium nitrate levels and to underestimate the organic aerosol concentration. For the calculation of organic mass concentration, we assumed OA/OC = 1.4 (Russell, 2003).

4.4 Comparison to Zeppelin measurements

The Zeppelin measurements were taken every 3 minutes in different heights, while the model predictions are every 15 minutes. To compare the results, the model output was interpolated to the times of the Zeppelin measurement periods. Figure S8 shows the comparison between model predictions and Zeppelin measurements of N_{10} and N_{100} (averages of 2000 points). PMCAMx-UF reproduced more than 80% of the 3-minute N_{10} data of Zeppelin within a factor of 2.

Figure 9 shows the predicted and observed vertical concentration profiles of particle number concentrations for N_{10} and N_{100}, calculated for 80 m altitude bins, averaged over the entire PEGASOS campaign. The average profile is the result of averaging of the 3-min measurements and interpolated predictions from different flights and heights. The model showed a small tendency to underpredict N_{10}, especially at heights between 200 and 400 m. PMCAMx-UF reproduced very well the N_{100} concentration at all heights (except for heights between 200 and 500 m). The average measured N_{10} at all heights was 6050 cm^{-3}, while the predicted concentration was equal to 5250 cm^{-3}. The model also reproduced 75% of the 3-min N_{100} Zeppelin measurements within a factor of 2. The measured average N_{100} at all heights was 1520 cm^{-3} and while the extended PMCAMx-UF predicted 1380 cm^{-3}. The ability of the revised model to reproduce reasonably well the high-time resolution Zeppelin measurements at different altitudes and locations is encouraging.

The vertical profiles shown are averages of different flights on different days and different altitudes for each flight. The number of samples at different altitudes changed for each flight creating additional variability in the measured profiles. There are relatively few measurements at higher altitudes (above 600 m) which took place in periods with relatively high concentrations, creating the apparent bump in the measurements. The model captured these high concentration

periods so it predicted the same bump for the average N_{100} concentration profile. This resulted in the peak at 750 m in Figure 9b. The model predictions are for the same periods and the same altitudes, and it is the reason why the model can reproduce the apparent N_{100} high concentration layer.

4.5 Effect of SOA formation on PMCAMx-UF performance

The results of the simulation without SOA condensation were also compared to the measurements. Including the SOA condensation reduced the NMB of N_{10} by 10%. The maximum decrease of N_{10} due to organics condensation appeared at noon when nucleation events took place. The maximum decrease of N_{10} due to organics condensation appeared at noon when nucleation events took place. Simulation of the secondary organics reduced the NMB of N_{100} from -40% to -20%, and the NME from -45% to -40%. The organic condensation increased the average condensation sink from 3.5×10^{-3} s^{-1} to 4.2×10^{-3} s^{-1}. The addition of organics species decreased the average of N_{10} from 6550 cm^{-3} to 6060 cm^{-3} (average observed N_{10} was 3910 cm^{-3}) while increasing the average of N_{100} from 750 cm^{-3} to 930 cm^{-3} (average observed N_{10} was 1080 cm^{-3}) (Tables 1-3).

Simulation of organics condensation improved the average predicted N_{100} at all heights in the Po Valley compared to Zeppelin measurements, by reducing the underprediction of N_{100} from 22% to 10% (Fig S10). The model with organics reproduced the measured N_{10} well at most heights, with the exception of the heights between 200 and 400 m (Fig S11a). At all heights, the predicted N_{100} with organics was closer to the measurements than the prediction of N_{100} without organics (Fig S11b).

4.6 Sensitivity to boundary conditions and emissions

The boundary conditions and emissions (gas and particles) represent potential sources of uncertainty in the particle number concentration predictions by PMCAMx-UF. Eight sensitivity simulations were conducted in which: (i) PM boundary concentrations were reduced by 50%, (ii) the boundary concentrations for all gases were reduced by 50%, (iii) the SO_2 boundary conditions were reduced by 50%, (iv) the SO_2 boundary conditions were set equal to zero, (v) the PM emissions at all sizes were reduced by 50%, (vi) the emissions of all gases were reduced

by 50%, (vii) the SO_2 emissions were reduced by 50%, and (viii) the SO_2 emissions were set equal to zero.

Table S7 shows the predicted domain-average change (%) of particle number concentrations due to these reductions in emissions and boundary conditions. The effect of the changes in boundary conditions by 50% was less than 5% for all cases, showing that the boundary conditions were not a major driver of the simulation. On the other hand, the emissions of sulfur dioxide, other vapors and particles had a major effect with changes of 10-35% for corresponding 50% emission changes. Setting the sulfur dioxide emissions to zero resulted in changes of 40-70% in the concentrations in the different particle size ranges showing its importance for new particle formation and growth during this photochemically active period.

5. Conclusions

A new version of PMCAMx-UF was developed including the condensation of organic vapors on ultrafine particles, using the volatility basis set framework. We evaluated the model predictions against field observations collected in Europe, for 34 days during June 5 to July 8, 2012. The measurements included both ground stations across Europe and airborne measurements from a Zeppelin. The goal of this work was to better understand the effect of condensation of semi-volatile organic vapors on regional aerosol number concentration in Europe during a photochemically active period.

Including organic condensation in PMCAMx-UF improved its ability to reproduce the concentration of particles larger than 10 nm (N_{10}) at ground level. The inclusion of organics decreased the NMB of N_{10} from 85% to 75% and the corresponding NME from 100% to 90%. However, the revised model still tends to overpredict N_{10} for the majority of the locations. This overprediction of N_{10} is due to the overprediction of nucleation in some sites and the low number concentration of predicted pre-existing particles (low condensational sink) and consistently low coagulation rate.

The N_{100} predictions by PMCAMx-UF were encouraging in most sites. The NMB of N_{100} was reduced from -40% to -20% after the addition of SOA condensation while the corresponding NME was reduced from 45% to 40%. This underprediction of N_{100} at all sites implies the need of improvement of either the size distribution of the emissions, and/or number of pre-existing

particles (condensation sink), and/or the addition of chemical aging of semi-volatile, and/or the effect of extremely low volatility organic vapors in the model (Patoulias et al., 2015).

The condensation of organics decreased the predicted N_{10} concentration across Europe. The condensation of organics both grew ultrafine particles and increased the probability of collision of fresh particles with large particles (coagulation sink). This change dominated over the faster growth of the fresh particles to larger sizes in many, but not all, locations. The larger reduction of N_{10} due to organic condensation (25%) was predicted over Russia, Turkey, Eastern Europe and the Balkans. The SOA condensation increased the number of particles larger than 100 nm (N_{100}) in all locations. This predicted increase was more than 80% in northern Scandinavia and northern Russia.

Compared to the PEGASOS Zeppelin measurements in Po Valley, PMCAMx-UF reproduced the average N_{10} with an error less than 10% and N_{100} with less than 10% at all heights up to 1000 m. The model with the condensation of organics performed better than the one without organics, in reproducing the observed vertical profile of both N_{10} and N_{100}. The model with organics reproduced more than 85% and 75% of 3 min data of Zeppelin within a factor of 2 for N_{10} and N_{100}, respectively.

The increase of N_{100} concentrations and the decrease of N_{10} concentrations in most areas due to the formation of semivolatile organic aerosol during this photochemically active period represent two of the major insights offered by these simulations. As expected, better simulation of the formation and partitioning of organic compounds closes the gap between observations and predictions of particle number distributions. The complex role of chemical aging reactions but also LVOC and ELVOC formation (Ehn et al., 2014; Tröstl et al., 2016), that have been neglected in this study, will be the topic of a forthcoming publication.

Acknowledgements: We thank Markus Fiebig, Chris Lunder, Pasi Aalto, Hans Karlsson, Erik Swietlicki, Moa Sporre, Jean-Philippe Putaud, Colin O'Dowd, Ciaran Monahan, Kay Weinhold, Wolfram Birmili, Andre Sonntag, Harald Flentje, Thomas Tuch, Alfred Wiedensohler, Bourrianne Thierry, Greg Roberts and Johannes Größ and Evangelia Kostenidou, Nikolaos Mihalopoulos, Giorgos Kouvarakis, George Biskos, and Spiridon Bezantakos for the measurements. All measurement presented here are from the Chemistry- Aerosol Mediterranean Experiment project (ChArMEx, http://charmex.lsce.ipsl.fr), which is the atmospheric component

of the French multidisplinary program MISTRALS (Mediterranean Integrated Studies aT Regional And Local Scales). ChArMEx-France was principally funded by INSU, ADEME, ANR, CNES, CTC (Corsica region), EU/FEDER, Météo-France, and CEA.This work was funded by the ARISTEIA project (National Research Excellence 490 Grant) and the ATMOPACS project (grant agreement 267099).

6. References

Adams, P.J., Seinfeld, J. H.: Predicting global aerosol size distributions in general circulation models, J. Geophys. Res., 107, 4370, 2002.

Anttila, T., Kerminen, V.: Condensational growth of atmospheric nuclei by organic vapours, J. Aerosol Sci., 34, 41–61, 2003.

Argueso, D, Hidalgo-Munoz, J. M., Gamiz-Fortis, S. R., and Esteban-Parra, M. J.: Evaluation of WRF parameterizations for climate studies over Southern Spain using a multistep regionalization, J. Climate, 24, 5633–5651, 2011.

Baranizadeh, E., Murphy, B. N., Julin, J., Falahat, S., Reddington, C. L., Arola, A., Ahlm, L., Mikkonen, S., Fountoukis, C., Patoulias, D., Minikin, A., Hamburger, T., Laaksonen, A., Pandis, S. N., Vehkamäki, H., Lehtinen, K. E. J., and Riipinen, I.: Implementation of state-of-the-art ternary new-particle formation scheme to the regional chemical transport model PMCAMx-UF in Europe, Geosci. Model Dev., 9, 2741-2754, 2016.

Carter, W. P. L.: Programs and files implementing the SAPRC-99 mechanism and its associates emissions processing procedures for Models-3 and other regional models, January 31, 2000.

Dal Maso, M., Kulmala M., Riipinen, I., Wagner, R., Hussein, T., Aalto, P. and Lehtinen, K. E. J.: Formation and growth of fresh atmospheric aerosols: eight years of aerosol size distribution data from SMEAR II, Hyytiälä, Finland, Boreal Env. Res., 10, 323–336, 2005.

de Meij, A., Gzella, A., Cuvelier, C., Thunis, P., Bessagnet, B., Vinuesa, J. F., Menut, L., and Kelder, H. M.: The impact of MM5 and WRF meteorology over complex terrain on CHIMERE model calculations, Atmos. Chem. Phys., 9, 6611– 6632, 2009.

Denier van der Gon, H. A. C., Visschedijk, A. J. H., Johansson, C., Hedberg Larsson, E., Harrison, R., and Beddows, D.: Size resolved pan European anthropogenic particle number

582 inventory, EUCAARI Deliverable report D141 (available on request from EUCAARI
583 project office), TNO, the Netherlands, 2009.
584 Donahue, N. M., Robinson, A. L., Stanier, C. O., and Pandis, S. N.: Coupled partitioning,
585 dilution, and chemical aging of semivolatile organics, Environ. Sci. Technol., 40, 2635–
586 2643, 2006.
587 Ehn, M., Thornton, J. A., Kleist, E., Sipilä, M., Junninen, H., Pullinen, I., Springer, M., Rubach,
588 F., Tillmann, R., Lee, B., Lopez- Hilfiker, F., Andres, S., Acir, I. H., Rissanen, M., Jokinen,
589 T., Schobesberger, S., Kangasluoma, J., Kontkanen, J., Nieminen, T., Kurtén, T., Nielsen,
590 L. B., Jørgensen, S., Kjaergaard, H. G., Canagaratna, M., Dal Maso, M., Berndt, T., Petäjä,
591 T., Wahner, A., Kerminen, V. M., Kulmala, M.,Worsnop, D. R.,Wildt, J., and Mentel, T.
592 F.: A large source of low-volatility secondary organic aerosol, Nature, 506, 476–479, 2014.
593 Eisele, F. L. and McMurry, P. H.: Recent progress in understanding particle nucleation and
594 growth, Phil. Trans. Royal Soc. London, 352, 191-201, 1997.
595 Environ, User's guide to the comprehensive air quality model with extensions (CAMx), version
596 4.02, report, ENVIRON Int. Corp., Novato, CA, 2003.
597 Fountoukis, C., Megaritis, A. G., Skyllakou, K., Charalampidis, P. E., Pilinis, C., Denier van der
598 Gon, H. A. C., Crippa, M., Canonaco, F., Mohr., C., Prévôt, A. S. H., Allan, J. D., Poulain,
599 L., Petäjä, T., Tiitta, P., Carbone, S., Kiendler-Scharr, A., Nemitz, E., O'Dowd, C.,
600 Swietlicki, E., and Pandis, S.N.: Organic aerosol concentration and composition over
601 Europe: Insights from comparison of regional model predictions with aerosol mass
602 spectrometer factor analysis, Atmos. Chem. Phys., 14, 9061 - 9076, 2014.
603 Fountoukis, C., Riipinen, I., Denier van der Gon, H. A. C., Charalampidis, P. E., Pilinis, C.,
604 Wiedensohler, A., O'Dowd, C., Putaud, J. P., Moerman, M., and Pandis, S. N.: Simulating
605 ultrafine particle formation in Europe using a regional CTM: contribution of primary
606 emissions versus secondary formation to aerosol number concentrations, Atmos. Chem.
607 Phys., 12, 8663-8677, 2012.
608 Fountoukis, C., Racherla, P. N., Denier van der Gon, H. A. C., Polymeneas, P., Charalampidis,
609 P. E., Pilinis, C., Wiedensohler, A., Dall'Osto, M., O'Dowd, C., and Pandis, S. N.:
610 Evaluation of a three-dimensional chemical transport model (PMCAMx) in the European
611 domain during the EUCAARI May 2008 campaign, Atmos. Chem. Phys., 11, 10331–
612 10347, 2011.

613 Garcia-Diez, M., Fernandez, J., Fita, L., and Yague, C.: Seasonal dependence of WRF model
614 biases and sensitivity to PBL schemes over Europe, Q. J. Roy. Meteor. Soc., 139, 501–514,
615 2012.
616 Gaydos, T., Pinder, R., Koo, B., Fahey, K., Yarwood, G., and Pandis, S. N.: Development and
617 application of a three-dimensional Chemical Transport Model, PMCAMx, Atmos.
618 Environ., 41, 2594–2611, 2007.
619 Gaydos, T.M., Stainer, C.O., Pandis, S.N.: Modeling of insitu ultrafine atmospheric particle
620 formation in the eastern United State, J. Geophys. Res., 110, D07S12,
621 doi:10.1029/2004JD004683, 2005.
622 Goldstein, A. H. and Galbally, I. E.: Known and unexplored organic constituents in the earth's
623 atmosphere, Environ. Sci. Technol., 41, 1514–1521, 2007.
624 Guenther, A., Karl, T., Harley, P., Wiedinmyer, C., Palmer, P. I., and Geron, C.: Estimates of
625 global terrestrial isoprene emissions using MEGAN (Model of Emissions of Gases and
626 Aerosols from Nature), Atmos. Chem. Phys., 6, 3181–3210, 2006.
627 Hallquist, M., Wenger, J. C., Baltensperger, U., Rudich, Y., Simpson, D., Claeys, M., Dommen,
628 J., Donahue, N. M., George, C., Goldstein, A. H., Hamilton, J. F., Herrmann, H.,
629 Hoffmann, T., Iinuma, Y., Jang, M., Jenkin, M. E., Jimenez, J. L., Kiendler-Scharr, A.,
630 Maenhaut, W., McFiggans, G., Mentel, T. F., Monod, A., Prevot, A. S. H., Seinfeld, J. H.,
631 Surratt, J. D., Szmigielski, R., and Wildt, J.: The formation, properties and impact of
632 secondary organic aerosol: current and emerging issues, Atmos. Chem. Phys., 9, 5155–
633 5236, 2009.
634 Hamed, A., Joutsensaari, J., Mikkonen, S., Sogacheva, L., Dal Maso, M., Kulmala, M., Cavalli,
635 F., Fuzzi, S., Facchini, M. C., Decesari, S., Mircea, M., Lehtinen, K. E. J., and Laaksonen,
636 A.: Nucleation and growth of new particles in Po Valley, Italy, Atmos. Chem. Phys., 7,
637 355-376, 2007.
638 Im, U., Markakis, K., Unal, A., Kindap, T., Poupkou, A., Incecik, S., Yenigun, O., Melas, D.,
639 Theodosi, C., and Mihalopoulos, N.: Study of a winter PM episode in Istanbul using the
640 high resolution WRF/CMAQ modeling system, Atmos. Environ., 44, 3085-3094, 2010.
641 Jimenez, J. L., Canagaratna, M. R., Donahue, N. M., Prevot, A. S. H., Zhang, Q., Kroll, J. H.,
642 DeCarlo, P. F., Allan, J. D., Coe, H., Ng, N. L., Aiken, A. C., Docherty, K. S., Ulbrich, I.
643 M., Grieshop, A. P., Robinson, A. L., Duplissy, J., Smith, J. D., Wilson, K. R., Lanz, V. A.,

Hueglin, C., Sun, Y. L., Tian, J., Laaksonen, A., Raatikainen, T., Rautiainen, J., Vaattovaara, P., Ehn, M., Kulmala, M., Tomlinson, J. M., Collins, D. R., Cubison, M. J., E, Dunlea, J., Huffman, J. A., Onasch, T. B., Alfarra, M. R., Williams, P. I., Bower, K., Kondo, Y., Schneider, J., Drewnick, F., Borrmann, S., Weimer, S., Demerjian, K., Salcedo, D., Cottrell, L., Griffin, R., Takami, A., Miyoshi, T., Hatakeyama, S., Shimono, A., Sun, J. Y., Zhang, Y. M., Dzepina, K., Kimmel, J. R., Sueper, D., Jayne, J. T., Herndon, S. C., Trimborn, A. M., Williams, L. R., Wood, E. C., Middlebrook, A. M., Kolb, C. E., Baltensperger, U., and Worsnop, D. R.: Evolution of organic aerosols in the atmosphere, Science, 326, 1525–1529, 2009.

Jimenez-Guerrero, P., Jorba, O., Baldasano, J. M., and Gasso, S.: The use of a modelling system as a tool for air quality management: Annual high-resolution simulations and evaluation, Sci. Total Environ., 390, 323–340, 2008.

Jung, J., Fountoukis, C., Adams, P. J., and Pandis, S. N.: Simulation of in situ ultrafine particle formation in the eastern United States using PMCAMx-UF, J. Geophys. Res., 115, D03203, doi: 10.1029/2009JD012313, 2010.

Jung, J., Adams, P. J., and Pandis, S. N.: Evaluation of nucleation theories in a sulfur-rich environment, Aerosol Sci. Technol., 42, 495–504, 2008.

Jung, J., Adams, P. J., and Pandis, S. N.: Simulating the size distribution and chemical composition of ultrafine particles during nucleation events, Atmos. Environ., 40, 2248–2259, 2006.

Kanakidou, M., Seinfeld, J. H., Pandis, S. N., Barnes, I., Dentener, F. J., Facchini, M. C., Van Dingenen, R., Ervens, B., Nenes, A., Nielsen, C. J., Swietlicki, E., Putaud, J. P., Balkanski, Y., Fuzzi, S., Horth, J., Moortgat, G. K., Winterhalter, R., Myhre, C. E. L., Tsigaridis, K., Vignati, E., Stephanou, E. G., and Wilson, J.: Organic aerosol and global climate modelling: a review, Atmos. Chem. Phys., 5, 1053–1123, 2005.

Karydis, V. A., Tsimpidi, A. P., and Pandis, S. N.: Evaluation of a three-dimensional chemical transport model (PMCAMx) in the eastern United States for all four seasons, J. Geophys. Res., 112, doi: 10.1029/2006JD007890, 2007.

Kerminen, V.-M., Paramonov, M., Anttila, T., Riipinen, I., Fountoukis, C., Korhonen, H., Asmi, E., Laakso, L., Lihavainen, H., Swietlicki, E., Svenningsson, B., Asmi, A., Pandis, S. N., Kulmala, M., and Petäjä, T.: Cloud condensation nuclei production associated with

675 atmospheric nucleation: a synthesis based on existing literature and new results, Atmos.
676 Chem. Phys., 12, 12037-12059, 2012.
677 Kerminen, V.-M., Virkkula, A., Hillamo, R., Wexler, A. S., and Kulmala, M.: Secondary
678 organics and atmospheric cloud condensation nuclei production, J. Geophys. Res., 105,
679 9255–9264, 2000.
680 Kulmala, M., Asmi, A., Lappalainen, H. K., Baltensperger, U., Brenguier, J. L., Facchini, M. C.,
681 Hansson, H. C., Hov, O'Dowd, C. D., Pöschl, U., Wiedensohler, A., Boers, R., Boucher,
682 O., De Leeuw, G., Denier Van Der Gon, H. A. C., Feichter, J., Krejci, R., Laj, P.,
683 Lihavainen, H., Lohmann, U., McFiggans, G., Mentel, T., Pilinis, C., Riipinen, I., Schulz,
684 M., Stohl, A., Swietlicki, E., Vignati, E., Alves, C., Amann, M., Ammann, M., Arabas, S.,
685 Artaxo, P., Baars, H., Beddows, D. C. S., Bergström, R., Beukes, J. P., Bilde, M., Burkhart,
686 J. F., Canonaco, F., Clegg, S. L., Coe, H., Crumeyrolle, S., D'Anna, B., Decesari, S.,
687 Gilardoni, S., Fischer, M., Fjaeraa, A. M., Fountoukis, C., George, C., Gomes, L., Halloran,
688 P., Hamburger, T., Harrison, R. M., Herrmann, H., Hoffmann, T., Hoose, C., Hu, M.,
689 Hyvärinen, A., Hõrrak, U., Iinuma, Y., Iversen, T., Josipovic, M., Kanakidou, M.,
690 Kiendler-Scharr, A., Kirkevåg, A., Kiss, G., Klimont, Z., Kolmonen, P., Komppula, M.,
691 Kristjánsson, J. E., Laakso, L., Laaksonen, A., Labonnote, L., Lanz, V. A., Lehtinen, K. E.
692 J., Rizzo, L. V., Makkonen, R., Manninen, H. E., McMeeking, G., Merikanto, J., Minikin,
693 A., Mirme, S., Morgan, W. T., Nemitz, E., O'Donnell, D., Panwar, T. S., Pawlowska, H.,
694 Petzold, A., Pienaar, J. J., Pio, C., Plass-Duelmer, C., Prévôt, A. S. H., Pryor, S.,
695 Reddington, C. L., Roberts, G., Rosenfeld, D., Schwarz, J., Seland, O., et al.: General
696 overview: European Integrated project on Aerosol Cloud Climate and Air Quality
697 interactions (EUCAARI)-integrating aerosol research from nano to global scales, Atmos.
698 Chem. Phys., 11, 13061–130143, 2011.
699 Kulmala, M., Vehkamaki, H., Petaja, T., Dal Maso, M., Lauri, A., Kerminen, V.-M., Birmili, W.,
700 and McMurry, P. H.: Formation and growth of ultrafine atmospheric particles: A review of
701 observations, J. Aerosol Sci., 35, 143–176, 2004.
702 Kulmala, M., Pirjola, L., Makela, J.M.: Stable sulphate clusters as a source of new atmospheric
703 particles, Nature, 404, 66–69, 2000.
704 Kulmala, M., Toivonen, A., Makela, J. M., and Laaksonen A.: Analysis of the growth of
705 nucleation mode particles observed in Boreal forest, Tellus B, 50, 449-462, 1998.

706 Laakso, L., Makela, J. M., Pirjola, L., and Kulmala, M.: Model studies on ion – induced
707 nucleation in the atmosphere, J. Geophys. Res., 107, 4427, doi: 10.1029/2002JD002140,
708 2002.
709 Lane, T. E., Donahue, N. M., Pandis, S. N.: Simulating secondary organic aerosol formation
710 using the volatility basis-set approach in a chemical transport model, Atmos. Environ., 42,
711 7439– 7451, 2008a.
712 Lane, T. E., Donahue, N. M., Pandis, S. N.: Effect of NO*x* on secondary organic aerosol
713 concentrations, Environ. Sci. Technol., 42, 6022–6027, 2008b.
714 Makkonen, R., Asmi, A., Korhonen, H., Kokkola, H., Jarvenoja, S., Raisanen, P., Lehtinen, K. E.
715 J., Laaksonen, A., Kerminen, V.- M., Jarvinen, H., Lohmann, U., Bennartz, R., Feichter, J.,
716 and Kulmala, M.: Sensitivity of aerosol concentrations and cloud properties to nucleation
717 and secondary organic distribution in ECHAM5-HAM global circulation model, Atmos.
718 Chem. Phys., 9, 1747–1766, 2009.
719 Merikanto, J., Spracklen, D. V., Mann, G. W., Pickering, S. J., and Carslaw, K. S.: Impact of
720 nucleation on global CCN, Atmos. Chem. Phys., 9, 8601–8616, 2009.
721 Murphy, B. N. and Pandis, S.N.: Simulating the formation of semivolatile primary and secondary
722 organic aerosol in a regional chemical transport model, Environ. Sci. Technol., 43, 4722–
723 4728, 2009.
724 Napari, I., Noppel, M., Vehkamaki, H., and Kulmala, M.: Parameterization of ternary nucleation
725 rates for H_2SO_4-NH_3-H_2O vapors, J. Geophys. Res., 107, doi: 10.1029/2002JD002132,
726 2002.
727 Nenes, A., Pandis, S. N., and Pilinis, C.: ISORROPIA: a new thermodynamic equilibrium model
728 for multiphase multicomponent inorganic aerosols, Aquat. Geochem., 4, 123–152, 1998.
729 O'Dowd, C. D., Langmann, B., Varghese, S., Scannell, C., Ceburnis, D., and Facchini, M. C.: A
730 combined organic-inorganic sea-spray source function, Geophys. Res. Lett., 35, L01801,
731 2008.
732 Pandis, S. N., Wexler, A. S., and Seinfeld, J. H.: Secondary organic aerosol formation and
733 transport. 2. Predicting the ambient secondary organic aerosol size distribution, Atmos.
734 Environ., 27A, 2403–2416, 1993.

735 Pathak, R. K., Presto, A. A., Lane, T. E., Stanier, C. O., Donahue, N. M., Pandis, S. N.:
736 Ozonolysis of a-pinene: parameterization of secondary organic aerosol mass fraction,
737 Atmos. Chem. Phys., 7, 3811–3821, 2007.
738 Patoulias, D., Fountoukis, C., Riipinen, I., and Pandis, S. N.: The role of organic condensation on
739 ultrafine particle growth during nucleation events, Atmos. Chem. Phys., 15, 6337-6350,
740 2015.
741 Pierce, J. R. and Adams, P. J.: A computationally efficient aerosol nucleation/condensation
742 method: Pseudo-steady state sulfuric acid, Aerosol Sci. Technol., 43, 216–226, 2009.
743 Pirjola, L. and Kulmala, M.: Development of particle size and composition distributions with a
744 novel aerosol dynamics model, Tellus B, 53, 491–509, 2001.
745 Riipinen, I., Pierce, J. R., Yli-Juuti, T., Nieminen, T., Hakkinen, S., Ehn, M., Junninen, H.,
746 Lehtipalo, K., Petaja, T., Slowik, J., Chang, R., Shantz, N. C., Abbatt, J., Leaitch, W. R.,
747 Kerminen, V.-M., Worsnop, D. R., Pandis, S. N., Donahue, N. M., and Kulmala, M.:
748 Organic condensation: a vital link connecting aerosol formation to cloud condensation
749 nuclei (CCN) concentrations, Atmos. Chem. Phys., 11, 3865–3878, 2011.
750 Russell, L. M.: Aerosol organic-mass-to-organic-carbon ratio measurements, Environ. Sci.
751 Technol., 37, 2982–2987, doi:10.1021/Es026123w, 2003.
752 Skamarock, W. C., Klemp, J. B., Dudhia, J., Gill, D. O., Barker, D. M., Wang,W., and Powers, J.
753 G.: A Description of the Advanced Research WRF Version 2, NCAR Technical Note
754 (http://www.mmm.ucar.edu/wrf/users/docs/arw v2.pdf), 2005.
755 Sofiev, M., Vankevich, R., Lanne, M., Koskinen, J., and Kukkonen, J.: On integration of a Fire
756 Assimilation System and a chemical transport model for near-real-time monitoring of the
757 impact of wild-land fires on atmospheric composition and air quality, Modelling,
758 Monitoring and Management of Forest Fires, WIT Trans. Ecol. Envir., 119, 343–351,
759 2008a.
760 Sofiev, M., Lanne, M., Vankevich, R., Prank, M., Karppinen, A., and Kukkonen, J.: Impact of
761 wild-land fires on European air quality in 2006–2008, Modelling, Monitoring and
762 Management of Forest Fires, WIT Trans. Ecol. Envir., 119, 353–361, 2008b.
763 Sogacheva, L., Hamed, A., Facchini, M. C., Kulmala, M., and Laaksonen, A.: Relation of air
764 mass history to nucleation events in Po Valley, Italy, using back trajectories analysis,
765 Atmos. Chem. Phys., 7, 839-853, 2007.

Stanier, C. O., Pathak, R. K., and Pandis, S. N.: Measurements of the volatility of aerosols from α-pinene ozonolysis, Environ. Sci. Technol., 41, 2756–2763, 2007.

Stanier C. O., A. Y. Khlystov, and Pandis S. N.: Nucleation events during the Pittsburgh Air Quality Study: Description and relation to key meteorological, gas phase, and aerosol parameters, Aerosol Sci. Technol., 38S, 253-264, 2004.

Tröstl, J., Chuang, W. K., Gordon, H., Heinritzi, M., Yan, C., Molteni, U., Ahlm, L., Frege, C., Bianchi, F., Wagner, R., Simon, M., Lehtipalo, K., Williamson, C., Craven, J. S., Duplissy, J., Adamov, A., Almeida, J., Bernhammer, A.-K., Breitenlechner, M., Brilke, S., Dias, A., Ehrhart, S., Flagan, R. C., Franchin, A., Fuchs, C., Guida, R., Gysel, M., Hansel, A., Hoyle, C. R., Jokinen, T., Junninen, H., Kangasluoma, J., Keskinen, H., Kim, J., Krapf, M., Kürten, A., Laaksonen, A., Lawler, M., Leiminger, M., Mathot, S., Möhler, O., Nieminen, T., Onnela, A., Petäjä, T., Piel, F. M., Miettinen, P., Rissanen, M. P., Rondo, L., Sarnela, N., Schobesberger, S., Sengupta, K., Sipilä, M., Smith, J. N., Steiner, G., Tomè, A., Virtanen, A., Wagner, A. C., Weingartner, E., Wimmer, D., Winkler, P. M., Ye, P. L., Carslaw, K. S., Curtius, J., Dommen, J., Kirkby, J., Kulmala, M., Riipinen, I., Worsnop, D. R., Donahue, N. M., and Baltensperger, U.: The role of low-volatility organic compounds in initial particle growth in the atmosphere, Nature, 533, 527–531, 2016.

Tsimpidi, A. P., Karydis, V. A., Zavala, M., Lei, W., Molina, L., Ulbrich, I. M., Jimenez, J. L., and Pandis, S. N.: Evaluation of the volatility basis-set approach for the simulation of organic aerosol formation in the Mexico City metropolitan area, Atmos. Chem. Phys., 10, 525-546, 2010.

Tzivion, S., Feingold, G., and Levin, Z.: An efficient numerical solution to the stochastic collection equation, J. Atmos. Sci., 44, 3139–3149, 1987.

Tzivion, S., Feingold, G., and Levin, Z.: The evolution of raindrop spectra. Part II: collisional collection/breakup and evaporation in a rain shaft, Journal of the Atmospheric Sciences, 46, 3312–3327, 1989.

Vehkamaki, H., Kulmala, M., Napari, I., Lehtinen, K. E. J., Timmreck, C., Noppel, M., and Laaksonen, A.: An improved parameterization for sulfuric acid-water nucleation rates for tropospheric and stratospheric conditions, J. Geophys. Res., 107, 4622–4632, 2002.

795 Visschedijk, A. J. H., Zandveld, P., and Denier van der Gon, H. A. C.: TNO Report 2007 A-
796 R0233/B: A high resolution gridded European emission database for the EU integrated
797 project GEMS, Netherlands, Organization for Applied Scientific Research, 2007.
798 Wang, M. and Penner, J. E.: Aerosol indirect forcing in a global model with particle nucleation,
799 Atmos. Chem. Phys., 9, 239-260, 2009.
800 Weber, R. J., McMurry, P. H., Mauldin III, R. L., Tanner, D. J., Eisele, F. L., Clarke, A. D., and
801 Kapustin, V. N.: New particle formation in the remote troposphere: a comparison of
802 observations at various sites, Geophys. Res. Lett., 26, 307–310, 1999.
803 Weber, R. J., McMurry, P. H., Mauldin, L., Tanner, D. J., Eisele, F. L., Brechtel, F. J.,
804 Kreidenweis, S. M., Kok, G. L., Schillawski, R. D., and Baumgardner, D.: A study of new
805 particle formation and growth involving biogenic and trace gas species measured during
806 ACE 1, J. Geophys. Res., 103, 16385–16396, 1998.
807 Yu, F. and Luo, G.: Simulation of particle size distribution with a global aerosol model:
808 contribution of nucleation to aerosol and CCN number concentrations, Atmos. Chem.
809 Phys., 9, 7691– 7710, 2009.
810 Yue, D. L., Hu, M., Zhang, R. Y., Wang, Z. B., Zheng, J., Wu, Z. J., Wiedensohler, A., He, L.
811 Y., Huang, X. F., and Zhu, T.: The roles of sulfuric acid in new particle formation and
812 growth in the mega-city of Beijing, Atmos. Chem. Phys., 10, 4953-4960, 2010.Zhang,
813 K.M., Wexler, A.S.: A hypothesis for condensation of fresh atmospheric nuclei, J.
814 Geophys. Res., 107, 4577, 2002.
815
816

Table 1: Prediction skill metrics of PMCAMx-UF against daily ground measurements of particle number concentration with diameter above 10 nm from 16 stations during 5 June – 8 July 2012.

Station	Mean Observed	Mean Predicted (cm^{-3})		Normalized Mean Bias (NMB) (%)		Normalized Mean Error (NME) (%)	
		With Organics	Without Organics	With Organics	Without Organics	With Organics	Without Organics
				N_{10}			
ASP	2090	5533	5496	165	163	165	163
BIR	1937	4950	4608	156	138	160	143
COR	2994	6768	7455	126	149	126	149
FIN	3932	6091	6191	55	57	57	60
HOH	3809	3801	4155	0	9	36	40
HYY	2616	2239	2408	-14	-8	33	35
ISP	6307	10481	11420	66	81	78	91
KPU	5245	6686	8581	27	64	56	82
MAC	822	1965	1758	139	114	149	135
MEL	6045	7325	8680	21	44	60	75
PAT	4858	5333	5449	10	12	50	53
SCH	1286	2913	3279	127	155	127	155
SPC	8319	7398	8547	-11	3	34	33
THE	4022	9755	10334	143	157	143	160
VAV	3230	7561	7601	134	135	136	137
WAL	5036	8194	8852	63	76	74	85
ALL	**3909**	**6062**	**6551**	**75**	**85**	**90**	**100**

826 **Table 2:** Prediction skill metrics of PMCAMx-UF against daily ground measurements of particle
827 number concentration with diameter above 50 nm from 16 stations during 5 June – 8 July 2012.

Station	Mean Observed	Mean Predicted (cm^{-3})		Normalize Mean Bias (NMB) (%)		Normalized Mean Error (NME) (%)	
		With Organics	Without Organics	With Organics	Without Organics	With Organics	Without Organics
				N_{50}			
ASP	1353	2419	1835	79	36	81	47
BIR	1046	1364	1111	30	6	61	53
COR	2460	3155	2883	28	17	41	37
FIN	3085	4163	3905	35	27	39	32
HOH	1988	1550	1340	-22	-33	31	35
HYY	1546	1092	829	-29	-46	40	49
ISP	3500	5399	4728	54	35	70	56
KPU	2955	3674	3424	24	16	30	25
MAC	489	315	278	-36	-43	70	67
MEL	2243	2197	1824	-2	-19	23	24
PAT	3249	3211	2983	-1	-8	29	28
SCH	839	1202	1053	43	26	65	54
SPC	3235	3686	3300	14	2	29	23
THE	2334	5147	4545	120	95	120	95
VAV	1628	2192	1812	35	11	45	33
WAL	2050	2295	1882	12	-8	22	16
ALL	**2125**	**2691**	**2358**	**25**	**10**	**50**	**40**

828
829
830
831
832
833
834

Table 3: Prediction skill metrics of PMCAMx-UF against daily ground measurements of particle number concentration with diameter above 100 nm from 16 stations during 5 June – 8 July 2012.

Station	Mean Observed	Mean Predicted (cm^{-3})		Normalize Mean Bias (NMB) (%)		Normalized Mean Error (NME) (%)	
		With Organics	Without Organics	With Organics	Without Organics	With Organics	Without Organics
			N_{100}				
ASP	540	372	343	-31	-37	45	46
BIR	431	318	229	-26	-47	59	55
COR	1304	1180	914	-9	-30	37	36
FIN	1769	2002	1652	13	-7	29	22
HOH	911	558	448	-40	-50	43	51
HYY	736	309	207	-60	-70	60	70
ISP	1766	1461	1245	-17	-30	32	37
KPU	1526	1486	1228	-3	-20	28	25
MAC	242	116	86	-50	-64	60	65
MEL	998	671	484	-33	-51	38	51
PAT	1758	1471	1154	-16	-34	25	35
SCH	496	442	360	-11	-27	43	36
SPC	1667	1387	1132	-17	-32	31	37
THE	1398	2020	1649	45	18	53	40
VAV	749	438	358	-41	-52	46	54
WAL	924	577	464	-38	-50	39	50
ALL	**1076**	**926**	**747**	**-20**	**-40**	**40**	**45**

$$\text{NMB}=\sum_{i=1}^{n}(P_i-O_i)\Big/\sum_{i=1}^{n}O_i\ ;\qquad \text{NME}=\sum_{i=1}^{n}|P_i-O_i|\Big/\sum_{i=1}^{n}O_i$$

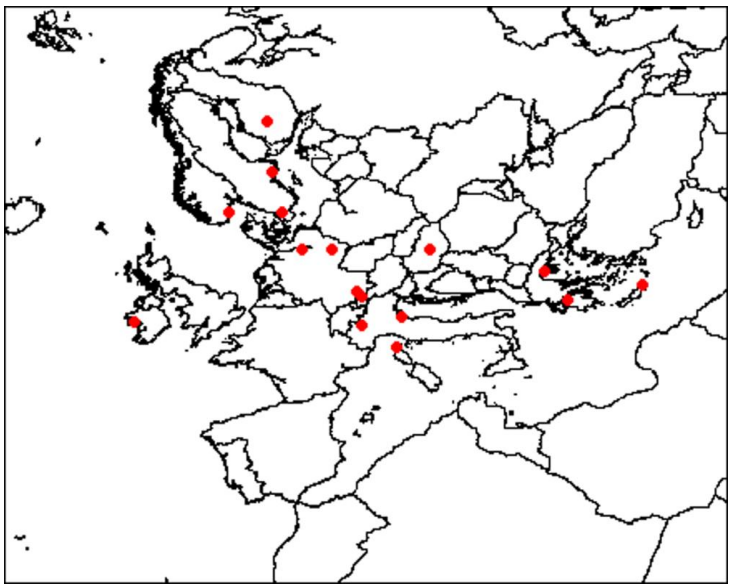

Figure 1: Modeling domain of PMCAMx-UF for Europe. Red dots show the measurement stations of Birkenes (Norway), Hyytiala (Finland), K-Puszta (Hungary), Aspvreten (Sweden), Vavihill (Sweden), Ispra (Italy), San Pietro Capofiume (Italy), Corsica (France), Patras (Greece), Finokalia (Greece), Thessaloniki (Greece), Mace Head (Ireland), Schneefernerhaus (Germany), Hohenpeissenberg (Germany), Melpitz (Germany) and Waldhof (Germany).

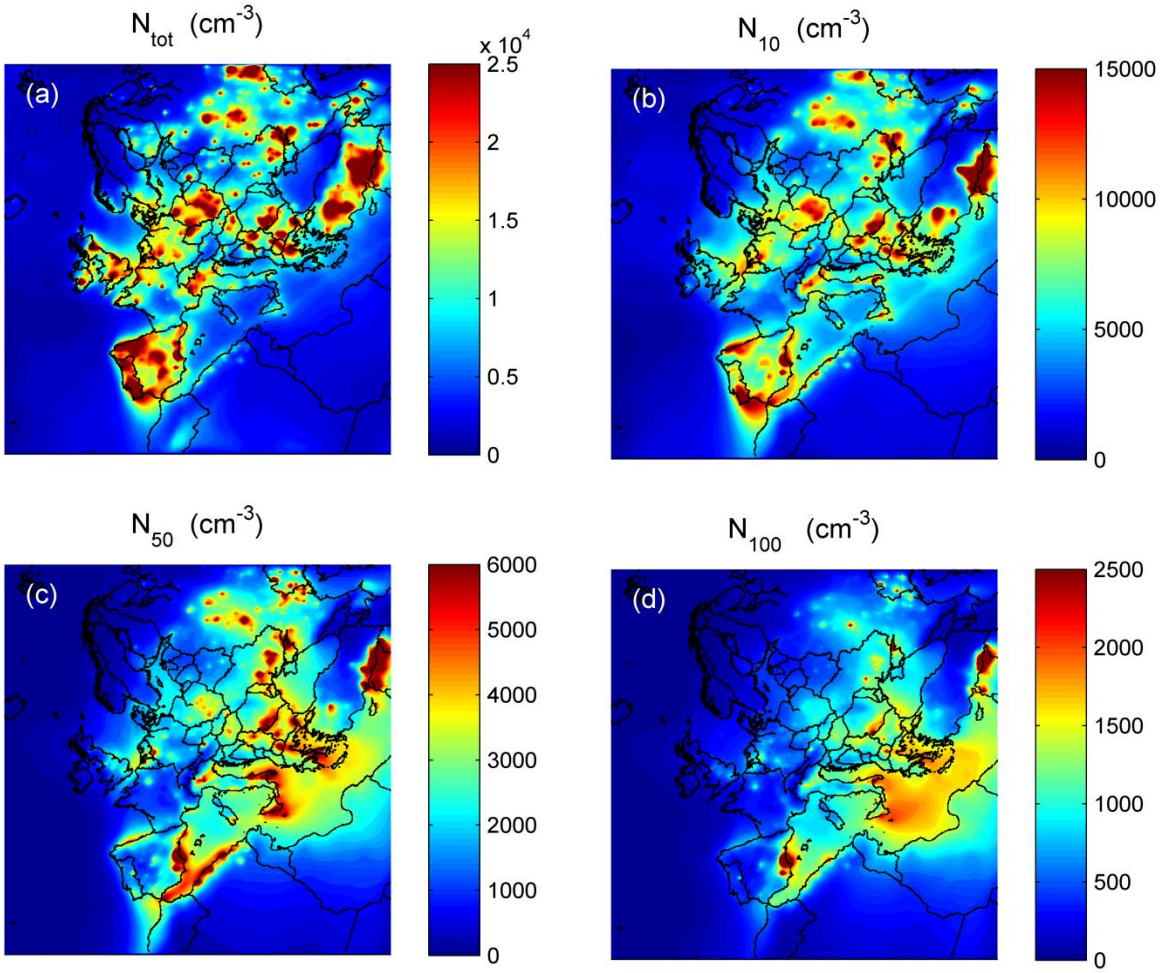

848

849

850 **Figure 2:** Ground level average number concentrations (cm^{-3}) predicted by the base case
851 simulation during 5 June – 8 July 2012 for: (a) all particles (N_{tot}); and particles above (b) 10 nm
852 (N_{10}); (c) 50 nm (N_{50}); and (d) 100 nm (N_{100}). Different color scales are used.

853

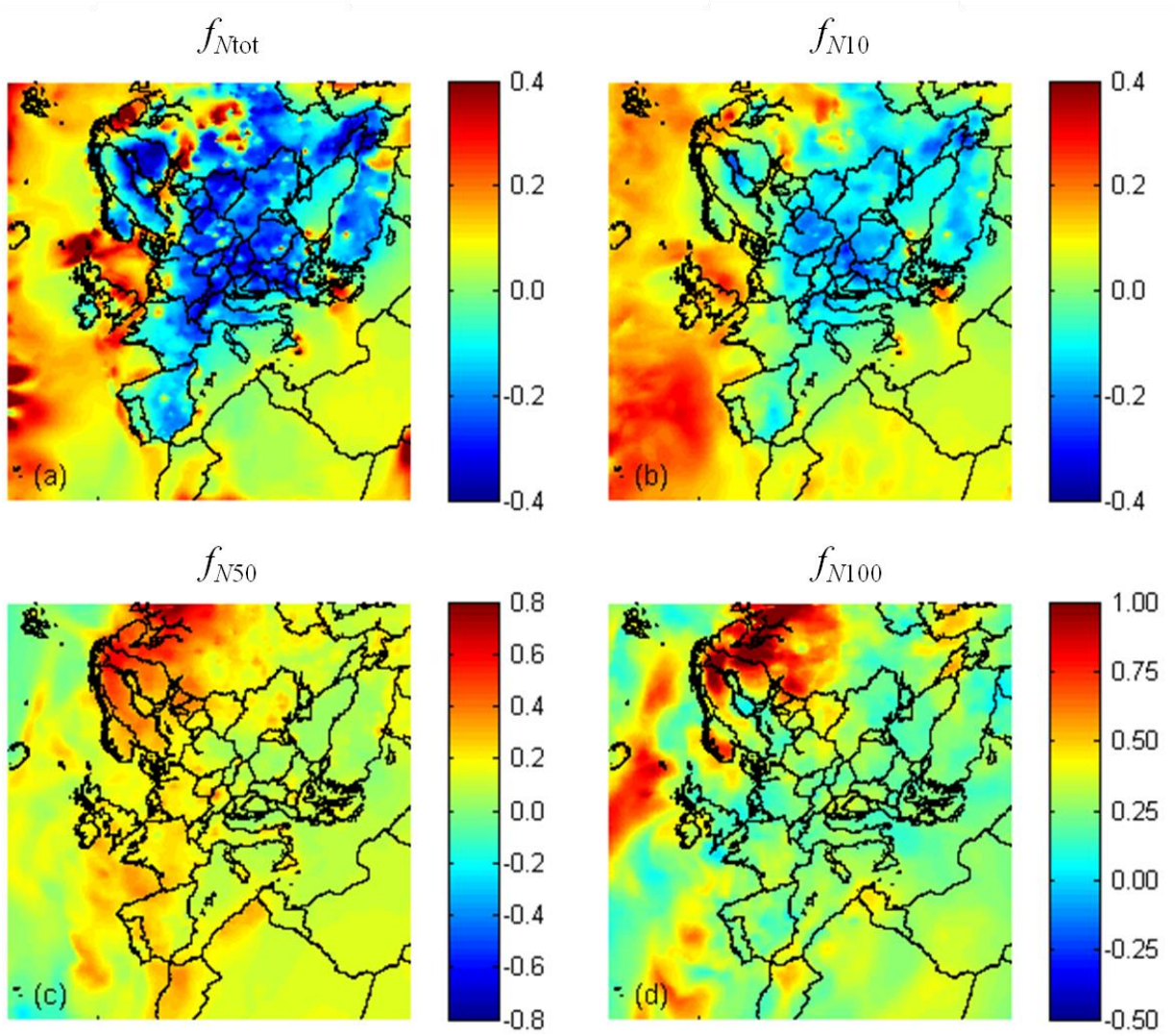

854

855

856 **Figure 3:** Ground level average fractional increase (f_{Nx}) of number concentration due to the
857 condensation of organic species predicted during 5 June – 8 July for: (a) all particles ($f_{N\mathrm{tot}}$);
858 particles above (b) 10 nm (f_{N10}); (c) 50 nm (f_{N50}); and (d) 100 nm (f_{N100}). Different scales are
859 used.

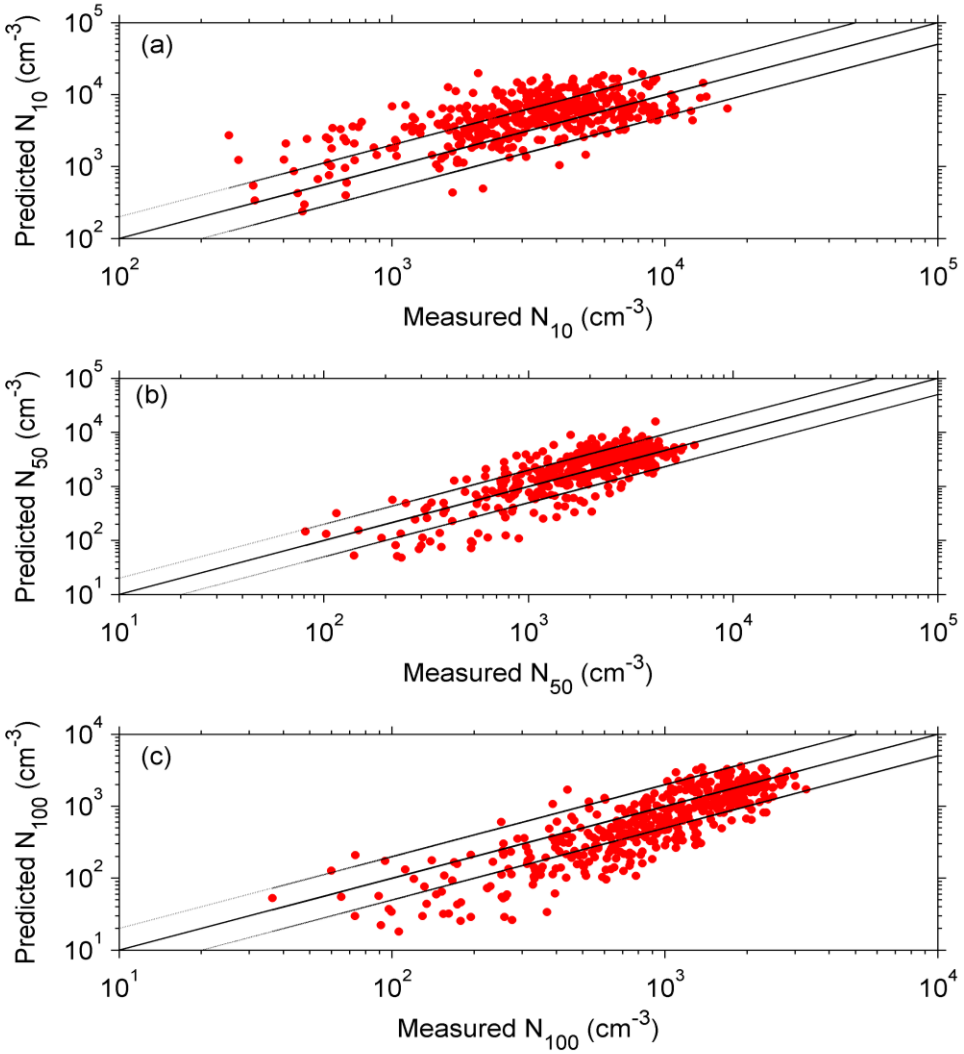

Figure 4: Comparison of predicted versus observed particle number concentrations (cm^{-3}) above 10, 50 and 100 nm from the 16 measurement stations across Europe during 5 June – 8 July 2012. Each point corresponds to a daily average value. Also shown the 1:1, 2:1 and 1:2 lines.

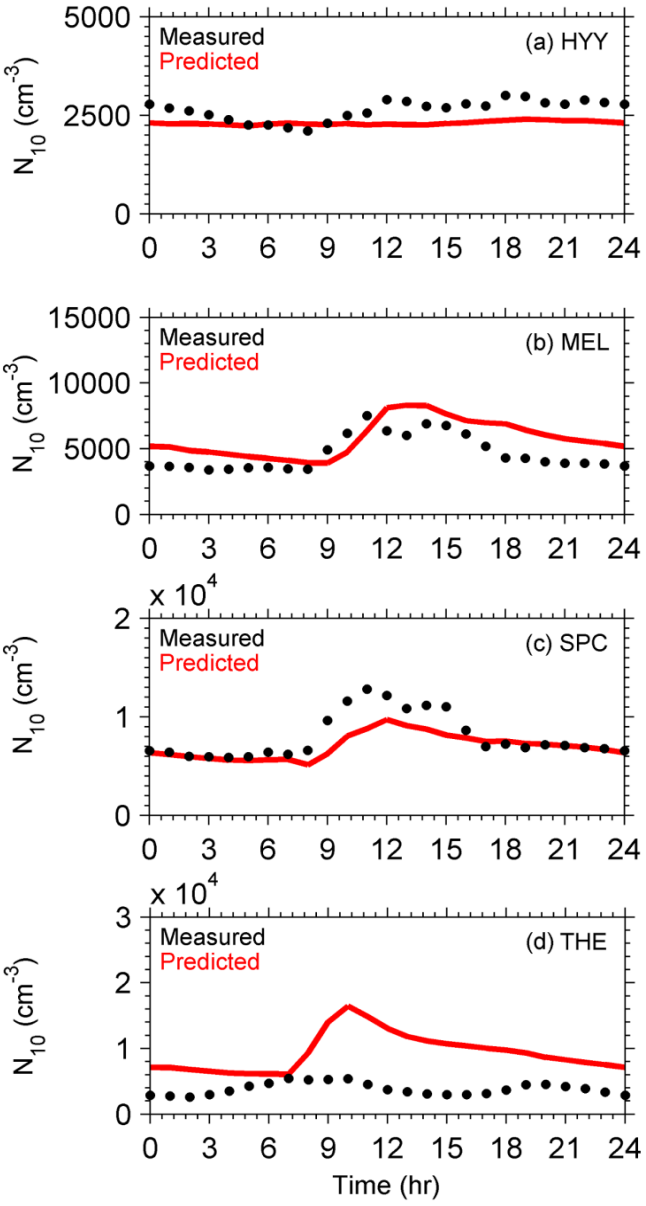

872

873

874 **Figure 5:** Average diurnal profiles of particle number concentrations (cm^{-3}) above 10 nm in: (a)
875 Hyytiala (Finland); (b) Melpitz (Germany); (c) San Pietro Capofiume (Italy) and (d)
876 Thessaloniki (Greece) during 5 June – 8 July 2012. Red lines correspond to predictions and black
877 symbols to observations.

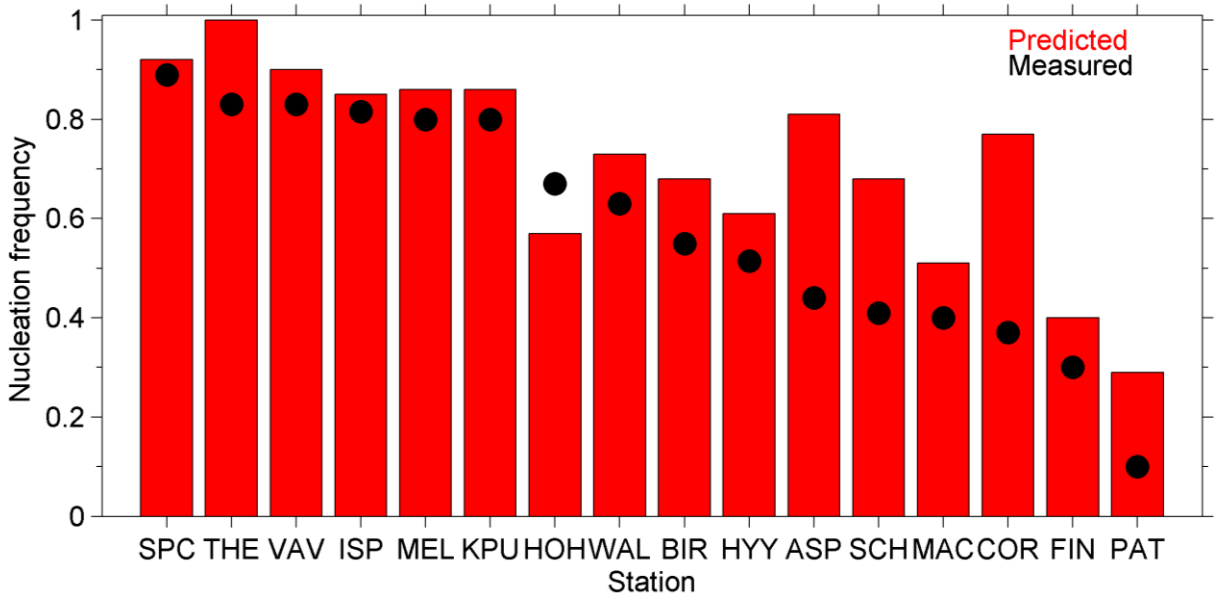

Figure 6: Predicted (red bars) vs. observed (black symbols) nucleation frequencies in the 16 measurement stations during 5 June – 8 July 2012.

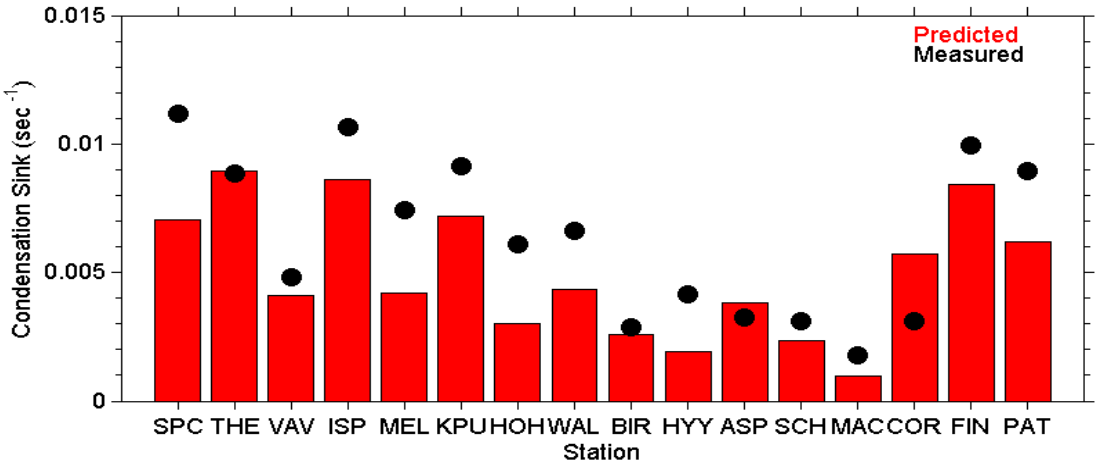

Figure 7: Predicted (red bars) vs. observed (black symbols) condensation sink in the 16 measurement stations during 5 June – 8 July 2012.

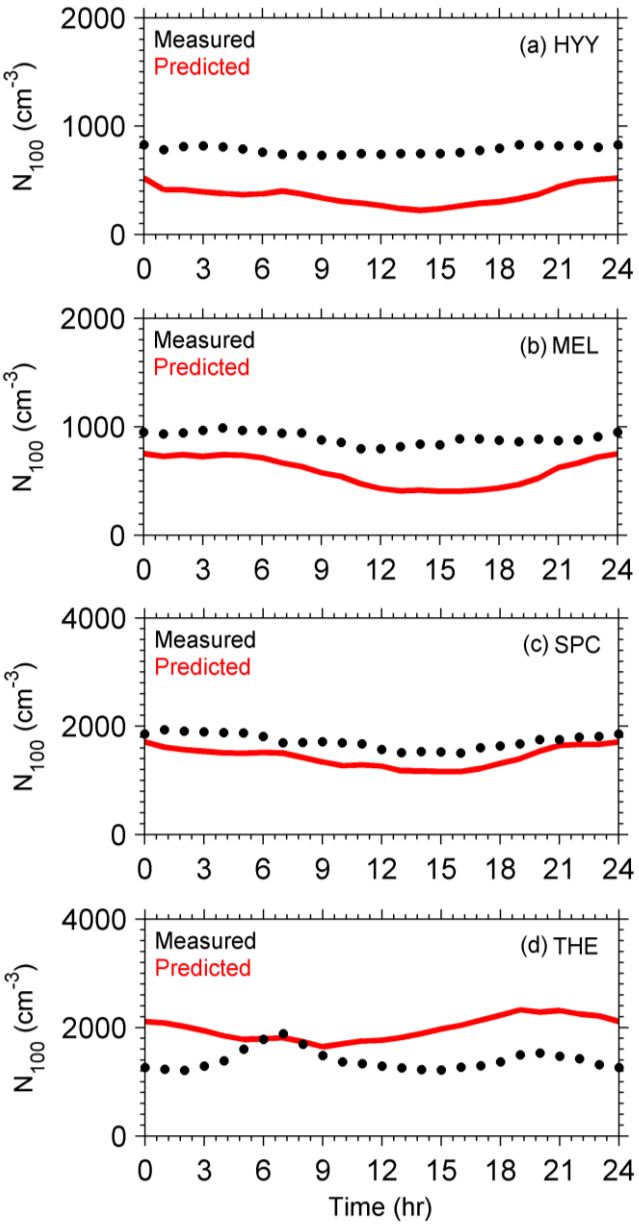

Figure 8: Average diurnal profiles of particle number concentrations (cm^{-3}) above 100 nm: in (a) Hyytiala (Finland); (b) Melpitz (Germany); (c) San Pietro Capofiume (Italy) and (d) Thessaloniki (Greece) during 5 June – 8 July 2012. Red lines correspond to predictions and black symbols to observations.

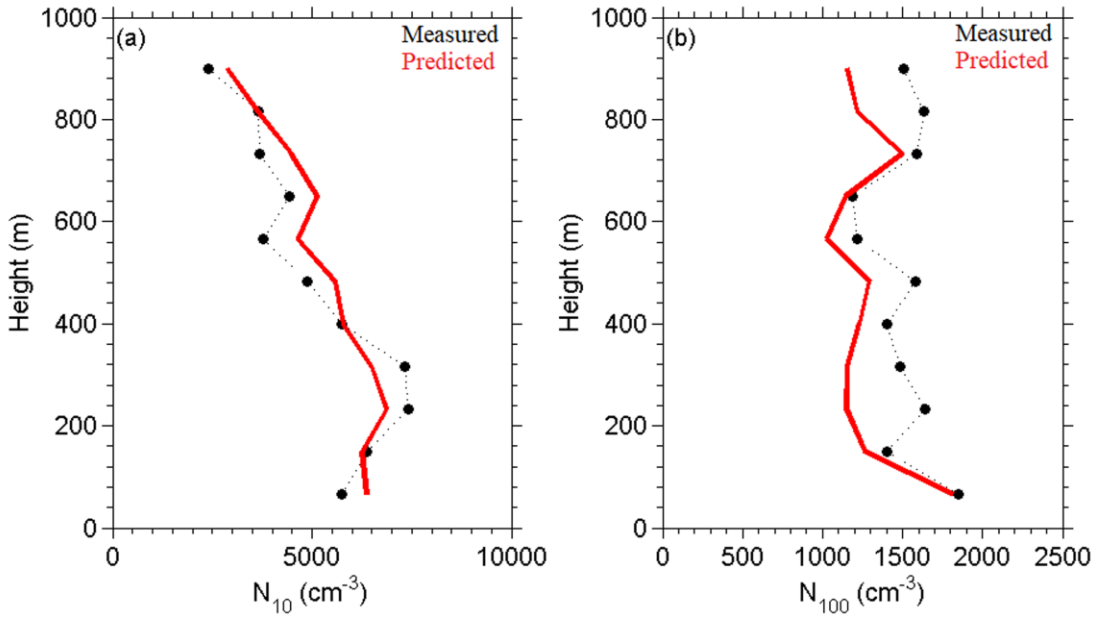

906

907 **Figure 9:** Comparison of predicted PMCAMx-UF (red line) vs. observed (black dots) vertical
908 profiles of averaged particle number concentrations for (a) N_{10} and (b) N_{100} of 25 flights over the
909 Po Valley during the PEGASOS campaign.

910

911